Alcohol Intoxication Effects on Visual Perception: An fMRI Study

V. D. Calhoun[§†*], D. Altschul[*], V. McGinty[*], R. Shih[*], D. Scott[*], G. D. Pearlson[§†*]

[§]Olin Neuropsychiatry Research Center, Institute of Living, Hartford, CT 06106.

[†]Dept. of Psychiatry, Yale University, New Haven, CT 06520

[*]Dept. of Psychiatry, Johns Hopkins University, Baltimore, MD 21205.

Originally submitted: NeuroImage: 11 December 2002

Revised version submitted: 19 March 2003

This version submitted: 14 May 2003

Manuscript Number: NIMG 314

Correspondence:

Vince Calhoun, Ph.D.

Olin Neuropsychiatry Research Center

Institute of Living

200 Retreat Ave.

Hartford, CT 06106

PH: 860-545-7768

E-mail: vince.calhoun@yale.edu

Abstract:

We examined the effects of two doses of alcohol (EtOH) on the fMRI activation during a visual perception task. The Motor-Free Visual Perception Test, Revised (MVPT-R) provides measures of overall visual perceptual processing ability. It incorporates different cognitive elements including visual discrimination, spatial relationships and mental rotation. We used the MVPT-R to study brain activation patterns in healthy controls sober, and at two doses of alcohol intoxication with event-related fMRI. The fMRI data were analyzed using a general linear model approach based upon a model of the time course and a hemodynamic response estimate. Additionally, a correlation analysis was performed to examine dose-dependent amplitude changes. With regard to alcohol-free task-related brain activation, we replicate our previous finding in which SPM group analysis revealed robust activation in visual and visual association areas, frontal eye field (FEF)/dorsolateral prefrontal cortex (DLPFC) and the supplemental motor area (SMA). Consistent with a previous study of EtOH and visual stimulation, EtOH resulted in a dose dependent decrease in activation amplitude over much of the visual perception network and in a decrease in the maximum contrast-to-noise-ratio (in the lingual gyrus). Despite only modest behavior changes (in the expected direction) significant dose-dependent activation increases were observed in insula, DLPFC, and precentral regions, whereas dose-dependent activation decreases were observed in anterior and posterior cingulate, precuneus, and middle frontal areas. Some areas (FEF/DLPFC/SMA) became more diffusely activated (i.e. increased in spatial extent) at the higher dose. Alcohol thus appears to have both global and local effects upon the neural correlates of the MVPT-R task, some of which are dose dependent.

Key Words: fMRI, functional, brain, visual perception, alcohol

INTRODUCTION

Visual perception has been investigated in skills such as object recognition (Sugio *et al.*, 1999), visual attention (Nakamura *et al.*, 2000), and examination of the visual properties of letters (Raij 1999). The Motor-Free Visual Perception Test, Revised (MVPT-R) (Colarusso and Hammill 1995) was designed to provide a reliable and valid measure of overall visual perceptual processing ability. It has been employed previously as a predictor of driving ability due to the following characteristics: (a) relevance to highway safety; (b) relation to on-the-road driving behavior or crashes; (c) capability of assessment on a driving simulator; and, (d) sensitivity to ETOH effects (Sivak *et al.*, 1981; Stokx and Gaillard 1986; Kaszniak *et al.*, 1991; Keyl *et al.*, 1997). As part of a larger study on simulated driving, we adopted the MVPT-R to an event-related fMRI paradigm. In that study, we demonstrated robust activation in ten healthy participants in visual and visual association areas, as well as frontal eye field areas/dorsolateral prefrontal cortex (FEF/DLPFC) and the supplemental motor area (SMA) (Calhoun *et al.*, 2001).

In the current study, we investigated the effect that two doses of alcohol had upon the neural correlates of visual perception that we identified previously. There have been few studies addressing the effect of alcohol on brain activity, and to our knowledge, no cognitive imaging studies were conducted at two or more alcohol doses.

The behavioral effects of alcohol intoxication are well known. In contrast to other drugs of abuse, it is widely believed that multiple extra-cellular signaling pathways are involved in the cognitive and behavioral effects of acute alcohol administration. Acute alcohol administration interferes with performance on neuropsychological tasks assessing a wide variety of cognitive processes, including immediate memory span (Tarter and Jones 1971; Jones 1973; Parker *et al.*, 1974), short-term memory (Rosen and Lee 1976; Tarter *et al.*, 1991), conceptual and abstracting

processes, and motor speed and coordination (Tarter and Jones 1971), which may relate to prefrontal cortex moderation of complex motor skills (Peterson *et al.*, 1990). Although some evidence suggests no alcohol-induced differences on attention tests (Tarter and Jones 1971), other findings indicate detrimental effects on attention allocation (Lamb and Robertson 1987). Learning and memory are also negatively affected by alcohol (Ryback 1971; Mungas *et al.*, 1994). In addition, psychophysical (Wegner *et al.*, 2001), and event-related potential (ERP) measures (Ahveninen *et al.*, 2000) are impaired by intoxication. An analysis of literature examining the P300 ERP response to alcohol challenge suggests slower information processing (Colrain *et al.*, 1993; Krull *et al.*, 1993). Neuropsychological and neurological deficits in executive function, visuospatial performance, and functions of gait and balance are detectable in alcoholic men even after a month of sobriety (Sullivan *et al.*, 2002b). Functions most severely affected in alcoholic women involve visuospatial and verbal and nonverbal working memory processes as well as gait and balance (Sullivan *et al.*, 2002b). In general, these studies support a deleterious effect of alcohol on cognitive functioning.

Despite the results just mentioned, there is relatively little imaging evidence examining how exposure to alcohol might transiently modulate brain function. A PET study found dose dependent blood flow decreases in cerebellum and increases (mostly at the higher dose) in right temporal and prefrontal regions (Volkow *et al.*, 1988). Alcohol is known to have vasoactive properties, confounding fMRI studies relying upon phenomenological hemodynamic changes. Global changes (more specifically decreases) in fMRI signal changes are likely confounded by such changes. A previous fMRI study reported that alcohol resulted in a significant activation decrease in visual areas, with slightly more right sided decreases (Levin *et al.*, 1998a).

There has been some work examining differences in brain activation between chronic alcoholics and healthy controls (Pfefferbaum *et al.*, 2001). In general, it is reported that frontal activity is modified in chronic alcohol users. On a working memory task, after controlling for baseline vigilance response, Tapert *et al.*, found decreases in the right superior and inferior parietal, right middle frontal, right postcentral, and left superior frontal cortex, (Tapert *et al.*, 2001). Another fMRI study suggested a reorganization of brain function resulting from long-term alcohol exposure and reported changes in working memory, decreases in Brodmann areas (BA) 9, 10, and 45 and increases in BA 47 (Pfefferbaum *et al.*, 2001). Neural correlates of alcohol craving have been reported in subcortical basal ganglia, amygdala, hippocampus (Schneider *et al.*, 2001), prefrontal (George *et al.*, 2001) and orbitofrontal regions (Wrase *et al.*, 2002). From the Wrase study, it is not clear that brain regions showing changes due to chronic alcohol use are the same as regions that demonstrate transient functional changes in response to acute alcohol.

Given previous findings, we expected to find a global effect of alcohol resulting in signal decrease, but in addition, we predicted local effects including possible increases due to increased effort in task performance. We hypothesized that frontal and cerebellar regions would exhibit the largest dose-dependent decrease and that additional frontal regions would show a dose-dependent increase. We also hypothesized that there would be a dose associated task performance decrease.

Healthy right-handed volunteers performed MVPT-R tasks presented during an fMRI scan session in an event-related manner (Friston *et al.*, 1998) followed by a second fMRI scan session fifteen minutes after ingesting a dose of alcohol measured to achieve a blood alcohol content (BAC) of 0.05% or 0.1%. For the MVPT-R task, as we reported previously (Calhoun *et*

al., 2001), participants were shown a test stimulus on a screen and were asked to identify from four choices, the figure that contained the test stimulus within it (see Figure 1). Following a choice response, a white asterisk was presented on a black background until the next set of stimuli, approximately seventeen seconds later. Event-related analyses were performed with a model-based approach utilizing a canonical hemodynamic response function.

METHODS

Participants

Study participants were 10 screened healthy men (N = 7) and women, aged 24.2 ± 5.8 years. Participants were screened with a complete physical and neurological examination and the SCAN interview (Janca *et al.*, 1994) to eliminate participants with Axis I psychiatric disorders. All participants had good visual acuity without correction, valid driver's licenses, and good driving records assessed by self report. A payment of thirty dollars (plus an addition ten dollars based upon their performance of a separate driving task) was provided at the completion of the study. The Johns Hopkins Institutional Review Board approved the protocol and written informed consent was provided by all participants. Each participant received either a placebo or a dose of beverage alcohol individualized to participant gender and body mass index, calculated using a published algorithm (Kapur 1989). The beverage was administered in a single-blind standardized fashion, diluted with fruit juice to a constant volume, served in a glass wrapped in an alcohol soaked cloth, and designed to produce a BAC of 0.05%, 0.10%, or zero. BAC's were determined immediately before and after the scan session, using a hand-held breath meter. Participants began their test sessions 15 minutes post beverage. Each participant was run in 2 separate sessions, on 2 separate days, randomly, one at each alcohol blood level, always

preceded by a run without alcohol. Following completion of each scan session participants were compensated for their time.

Experimental Paradigms

A timeline of the experimental paradigm along with an example figure is presented in Figure 1. Fifteen MVPT-R figures (approximately half the test battery) were presented an average of seventeen seconds apart using the computer program E-Prime (Psychology Software Tools, Inc.). A white asterisk on a black background was visible during the inter-stimulus intervals. For each item, a central test stimulus was presented above four other figures (one target and three distracters). The visual perceptual processing involved in selecting the target can be categorized into 1) spatial relationships, 2) visual discrimination, 3) figure-ground and, 4) visual closure. The target is, in some cases, hidden, rotated, darkened, or resized and thus incorporates a number of visual perceptual elements.

The four figures were arranged below the test stimulus numbered 1 through 4, from left to right, as in the MVPT-R test. The participants looked into a mirror to see a screen subtending approximately 25 degrees of visual field. The figures were back-projected onto the screen and the participant indicated his/her item choice by pressing a fiber-optically monitored button panel. Buttons 1 and 2 were controlled by the index and middle fingers of the right hand, respectively, and buttons 3 and 4 were controlled by the index and middle fingers of the left hand, respectively. The buttons were held with the number 1 closest to the head and the number 4 closest to the feet of the participants. All figures remained on the screen until a choice was made (an average of 5-6 seconds). We recorded reaction times as well as response accuracy for each item in all participants. Training included showing participants a sample figure from the test

battery prior to the task. Scripted instructions were provided and were also displayed on the projection screen prior to beginning the task.

Figure 1: Timeline of the MVPT-R fMRI Paradigm

Imaging parameters

Scans were acquired on a Philips NT 1.5 Tesla scanner at the Kennedy Krieger Institute in Baltimore, Maryland. A sagittal localizer scan was performed first, followed by a T_1-weighted anatomic scan (repeat time (TR)=500ms, echo time (TE)=30ms, field of view=24cm, matrix=256×256, slice thickness=5mm, gap=0.5mm) consisting of 18 slices through the entire brain including most of the cerebellum. Next, we acquired axial oblique functional scans over the same 18 slices consisting of a single-shot, echo-planar scan (TR=1s, TE=39ms, field of view=24cm, matrix=64×64, slice thickness=5mm, gap=0.5mm) obtained consistently over a 5-minute period for a total of 300 scans. Ten "dummy" scans were performed at the beginning to allow for longitudinal equilibrium, after which the paradigm was automatically triggered to start by the scanner.

Data Analysis

Preprocessing: The images were first corrected for timing differences between the slices using windowed Fourier interpolation to minimize the dependence upon the reference slice chosen (van de Moortele *et al.*, 1997; Calhoun *et al.*, 2000). Next, the data were imported into the Statistical Parametric Mapping software package, SPM99 (Worsley and Friston 1995). Data were motion corrected, spatially smoothed with a 6×6×10 mm Gaussian kernel, and spatially normalized into the standard space of Talairach and Tournoux (Talairach and Tournoux 1988).

The data were slightly sub-sampled to 3×3×5mm, resulting in 53×63×28 voxels. For display, slices 4-28 were presented.

Statistical Analysis: Data from each participant was entered into a general linear model "fixed effect" group analysis framework using SPM99. The statistical model, using the conventional SPM analysis, employed stimulus functions (consisting of the times when the figures were *presented* to the participants) convolved with the standard SPM99 canonical hemodynamic response function consisting of the sum of two gamma functions. Data were high-pass (drift removal) filtered by entering sinusoidal functions into the model up to a frequency of 1/34s as covariates and low-pass filtered by smoothing the data temporally with a 4s Gaussian kernel. The resultant statistics were height corrected for multiple comparisons to $p < 0.05$ using a method derived from Gaussian random field theory (Friston *et al.*, 1996). Individual analyses were also performed to verify that the trends seen in this "fixed effect" group analysis were also seen in each individual data set. Additionally, a secondary "random effects" analysis was performed on the individual analyses with similar results to the fixed effects analysis, suggesting these results are somewhat representative of the population as a whole (Woods 1996). For the random effects analysis, because of low degrees of freedom, a more liberal *corrected* threshold of $p<0.05$ which controls for the false discovery rate was used (Genovese *et al.*, 2002).

In order to examine dose-dependent differences, we performed a second-level (paired *t*-test) analysis of the fixed-effect contrasts between each EtOH dose and its baseline scan. That is, we compared the amplitude difference between the sober (S) and drug (D) conditions for the high (H) dose with the amplitude difference between the sober and intoxicated conditions for the low (L) dose, indicated as ($\Delta_{H\pm L}[D\text{-}S]$).We also performed a correlation analysis using the participants' own BAC levels, with similar results.

RESULTS

All participants performed well on the MVPT-R task having an 85% average correct response (within 5% of the norm) as summarized in Table 1. Incorrect and correct responses were treated as equivalent in the model because we were primarily interested in gross visual perceptual processing rather than differences in decision-making. We explored the effect of alcohol (EtOH) at two blood alcohol content levels on MVPT-R task performance. At the lower BAC (mean 0.041 ± 0.016), on 5-point analog scale (where 5 indicated maximal intoxication) participants indicated subjective intoxication of mean 1.0 ± 0.7 and at the higher BAC (mean 0.096 ± 0.040), participants self-rated intoxication of mean 3.1 ± 0.8. The difference on the subjective intoxication scores was highly significant (p<1e-6).

Within participants, median response times were calculated, and the group average of these values are also presented in Table 1. Participants receiving the low dose of alcohol tended (p<0.07) towards slightly decreased reaction time whereas participants receiving the high dose of alcohol slightly (p<0.08) increased in reaction time. With regard to alcohol-free task-related brain activation SPM group analysis revealed robust activation in visual and visual association areas, FEF/DLPFC and the supplemental motor area (SMA). EtOH resulted in a dose dependent decrease in activation amplitude over much (but not all) of the visual perception network including primary visual and visual association areas. This is evident upon visual inspection of Figure 2. Additionally, dose dependent increases were observed in bilateral insular regions.

Table 1: Individual accuracy rates and reaction times

The main effect SPM group analysis for 1) (mean) sober (colored red/orange), 2) low dose (colored blue/cyan), and 3) high dose (colored green/yellow) is displayed in Figure 2. Upon examination of estimated motion parameters, no participant was found to have moved more than 2mm. Consistent with our previous study (on an independent sample of participants), the SPM analysis revealed activation in visual and visual association areas as well as FEF/DLPFC and the SMA. A summary of the detected regions is provided in Table 2. At the highest dose, some regions (FEF/DLPFC/SMA) became more diffusely activated, *i.e.* at the given threshold, the cluster size in each of these regions was greater.

Figure 2: Main effect group maps for (mean) sober, low dose, and high dose conditions

Table 2: Summary of areas detected in the main effects analysis

We observed both global and local hemodynamic effects of alcohol. There was a global decrease evident both by visual inspection of Figure 2 and by examination of the maximum *t*-value in Table 2 (sober=13.64, low dose=11.49, high dose=7.56) located in the lingual gyrus for all doses. In addition to the global effects, there were also localized increases and decreases. In particular, the contrast-to-noise in frontal regions increased (relative to sober) at the low dose and decreased (relative to sober) in the high dose (see Figure 3).

Figure 3: Graphical view of CNR differences detected in the main effects analysis

For the correlation analysis, a small, but detectable, effect was observed at a threshold of $p<0.05$ (uncorrected) controlled for false positives with a contiguity filter of k=50 voxels. The largest dose-dependent decreases were observed in bilateral parietal visual areas such as precuneus and also in bilateral visual area MT (although this was not independently verified with visual cortical mapping). The largest cluster demonstrating a dose-dependent increase was observed in the precentral gyrus. Corresponding images are presented in Figure 4 and tabulated in Table 3.

Figure 4: EtOH blood alcohol content correlation maps and plots

Table 3: Summary of areas detected in the correlation analysis

As each of the two drug conditions was compared to a baseline scan acquired on the same day, it was important to verify the consistency of results in these scans. To determine the consistency of results in the pre-drug condition, an omnibus F-test was performed on the two sober-condition imaging sessions. At a threshold of $p<0.05$ (uncorrected), there were only a few voxels which survived, and none of these were in areas that survived the threshold in other analyses, thus supporting the robustness of the results from the fMRI experiment.

We performed an analysis examining the differential effect that alcohol has on the seven male participants compared with the three female participants. Overall the maps were quite similar (due possibly to our small sample size). Only a few areas were found to be differentially modulated by EtOH. At the high dose, males demonstrated a larger decrease in the right superior temporal gyrus [maximum at (51, -6, 5)]. At the low dose, females had a larger decrease in primary visual and visual association areas, suggesting that the low dose had a greater global effect on female than on male participants. Performance measures showed female performance less than male performance at baseline (median reaction time=3.62s for males vs. 4.26s for females). Performance decreases were greater for females than males (change in reaction time was -.16s and +0.59s for males and -.78s and +1.36 for females in the low dose and high dose, respectively). Thus both male and female participants showed a performance increase at the low dose and a performance decrease at the high dose. There was no difference in accuracy measures. Note than none of the male vs. female performance results were statistically significant due to the small number of female participants.

DISCUSSION

The MVPT-R provides an overall measure of visuospatial processing ability. In our previous study, we demonstrated that the MVPT-R activates a large network of regions involved in visual and spatial perception (Calhoun *et al.*, 2001). The goal of this study was to examine the modulatory effect that alcohol has upon the fMRI activation patterns associated with this task, as well as any behavior effects.

There have been few studies addressing the effect of alcohol on brain activity, and to our knowledge, no fMRI studies have been conducted using two or more dose levels of alcohol. Alcohol is known to have vasoactive properties, and a previous fMRI study reported that alcohol

resulted in a decrease in visual activation, with a slightly greater decrease on the right side (Levin *et al.,* 1998a). We hypothesized there would be a global decrease in CNR. Such a decrease is evident both by visual inspection of Figure 2 and by examination of the maximum *t*-value in Table 2 (sober=13.64, low dose=11.49, high dose=7.56). The regions that became more diffusely activated at the higher dose were primarily frontal (FEF/DLPFC/SMA). This is consistent with increased recruitment of frontal regions to maintain performance on the task in an impaired state. In addition to the global effects, there were also localized increases and decreases.

The CNR in frontal regions increased (relative to sober) at the low dose and decreased (relative to sober) in the high dose. This may indicate more active (but the same) frontal regions at the low dose of alcohol as participants attempt to perform the task during mild intoxication, whereas at the high dose, additional frontal regions are recruited and are activated less efficiently.

We hypothesized that frontal and cerebellar regions would exhibit a dose dependent decrease (Sullivan *et al.*, 2000). Consistent with our hypothesis, bilateral negative correlations were observed in frontal regions just anterior and superior to the frontal eye fields. In particular, the CNR in frontal regions increased (relative to sober) at the low dose and decreased (relative to sober) in the high dose. From Figure 3 it can thus be seen that there is an inverted U relationship between dose and activation for prefrontal regions. This may indicate more active (but the same) frontal regions at the low dose of alcohol as participants attempt to perform the task during mild intoxication, whereas at the high dose, additional frontal regions are recruited and are activated less efficiently. Contrary to our hypothesis, we observed no dose dependent decreases in cerebellar activation. Occipital and parietal visual areas demonstrated the largest dose-dependent

decreases (but the relationship was linear in this case). Though most of the primary visual cortex did not meet our significance criterion, there was a dose dependent trend in many of these areas. This is evident upon visual inspection of Figure 2.

Additionally regions demonstrated dose dependent decreases. We observed a dose-dependent decrease in regions consistent with visual area MT (VMT). VMT additionally revealed robust activation for the main effect of the MVPT-R task (see Figure 2). It was recently shown that area MT, an area primarily responsive to motion, is also responsible for processing shape (Kourtzi *et al.*, 2002), and hence may reflect the task performance.

The largest dose-dependent increases observed in medial prefrontal and precentral gyri were consistent with greater effort as the participant tried to overcome their impairment. Increases were also observed in the right insula, consistent with a PET study which found alcohol increases in right temporal and prefrontal regions (Volkow *et al.*, 1988). The same study also demonstrated decreased cerebellar metabolism. A dose-dependent increase was observed in the right precentral gyrus. It has been shown that EtOH produces a psychomotor performance deficit in a dose-dependent manner (Hiltunen 1997).

As sex differences in perceptual speed and visuospatial tasks have been documented (Kimura 2002) as well as BOLD signal differences due to hematocrit differences (Levin *et al.*, 1998b), we performed an analysis examining the differential effect that alcohol has on the seven male participants compared with the three female participants. Though the number of participants is insufficient to draw a general conclusion, we found that for $p < 0.001$ (uncorrected), males decreased more in the left superior temporal gyrus at the high dose, and at the lower dose, females decrease more in primary visual and visual association areas. No statistically significant performance difference was observed. This evidence suggests that global

changes were induced in female participants more so than the male participants. The BAC levels were slightly higher for females (0.038 for males and 0.041 for females) at the lower dose, and at the higher dose (0.084 for males and 0.108 for females). This evidence suggests that, though our main findings are the same for both male and female participants, there are potentially important sex differences which should be studied in a larger number of participants.

We also hypothesized that there would be a dose-related performance decrease. We found that low dose alcohol slightly ($p<0.07$) decreased reaction time whereas high dose alcohol slightly ($p<0.08$) increased reaction time. This is consistent with performance measures on a study of a simulated driving task in which low-dose recipients indicated an awareness of their intoxication and made an attempt to compensate (McGinty *et al.*, 2001). In the current study, participant self-reports at the lower dose of intoxication are consistent with an attempt to compensate at the lower dose. The high-dose was associated with increased reaction time but unimpaired accuracy, consistent with a study showing impairments in speed and efficiency but not accuracy of timing on a variety of motor performance measures (Sullivan *et al.*, 2002a). While it might have been interesting to explore the relationship between task performance and brain activation, such an analysis would require more participants and a greater degree of performance variability.

We chose the MVPTR task in the context of a larger study on simulated driving. For example, Rebok *et al.*, found that the MVPTR task helped predict simulated driving performance in elderly individuals, both healthy and with Alzheimer's disease (Rebok *et al.*, 1990; Rebok *et al.*, 1994). It is informative to consider which component of visual perception might be most implicated in such differences. The most behaviorally relevant component of this visual perception task is the attentional aspect, but this is conjecture. The current study provides a map

of the neural correlates involved in the MVPTR visual perception task as well as those involved regions which are modulated by alcohol. In our previous study of simulated driving in sober individuals, we extracted, in addition to visual and motor components, separate components which were 1) in attentional and error monitoring areas and 2) modulated by driving speed (Calhoun *et al.*, 2002). In addition, this prior MVPTR study revealed separate components for visual and parietal regions, presumably involved in attention and spatial processing (Calhoun *et al.*, 2001). In the future, we plan to explore directly the relationship between the driving and MVPTR tasks, and the impact of alcohol upon this relationship.

Limitations of the current study include the lack of additional types of imaging information (such as perfusion) in order to quantify the global effects of alcohol upon resting cerebral blood flow. Additionally as we scanned both the sober and the drug condition in a single scan session it was necessary to have the sober condition always precede the drug condition. We attempted to minimize the possibility of order effects by randomizing the order in which participants received the doses. A third scan session starting with the drug condition would have been useful in this regard. It is also possible that there may have been practice effects between the sober and the drug condition. However we did not find significant differences between the two sober conditions, nor were there systematic changes in performance over time. A larger test battery would have been useful for detecting behavioral changes in the scanner. However due to a desire to have novel stimuli during each session, and the limited number of MVPT-R templates, it was not possible to increase the number of stimuli.

The effects of EtOH are complicated and can differ depending upon whether one is on the ascending or descending limb of the BAC curve (Conrod *et al.*, 1997). It was for this reason we measured BAC before and after the scan session and attempted to scan participants as close

to peak BAC as possible. However, more frequent measurement of BAC would have been useful. It would have also been useful to have a third, higher dose of EtOH, since a trend towards behavioral decrements were observed only at the high dose. We would expect, in this case, to see greater dose-related decreases in frontal regions and increased amplitude changes in regions associated with the visual perception task.

Strengths of the current study include the measurement of fMRI activation at two doses of EtOH, thus enabling detection of dose dependent changes. Additionally, we were able to detect EtOH associated changes in both global and local fMRI activation during a visual perception task. Many of the areas detected were also detected in a previous study of simulated driving (Calhoun *et al.*, 2002). In the future, it would be useful to directly compare regional activation during the two tasks.

CONCLUSIONS

To summarize, we examined the neural correlates of a driving related visual perception task under conditions of alcohol intoxication. We replicate our previous finding that the MVPT-R test battery activates a large network of areas including primary visual, visual association, frontal, parietal, and cerebellar regions, similar to those activated in simulated driving (Calhoun *et al.*, 2002). Performance accuracy was consistent across all sessions, reaction time slightly decreased in the low dose condition and slightly increased in the high dose condition. Despite only modest behavior changes, albeit in the expected direction, significant dose-dependent correlations were observed in insula, DLPFC, and precentral regions consistent with greater task effort whereas dose-dependent decreases were observed in anterior and posterior cingulate, precuneus, and middle frontal areas. Some areas (FEF/DLPFC/SMA) became more diffusely activated (i.e. increased in spatial extent) at the highest dose. Alcohol thus appears to have both

global and local effects upon the neural correlates of the MVPT-R task, some of which are dose dependent. Dose dependent decreases were observed in bilateral parietal and bilateral visual association areas, increases were observed in bilateral insula.

ACKNOWLEDGEMENTS

The authors would like to thank Edie Sears for assistance in manuscript preparation. The research was support by funding from the Johns Hopkins Outpatient General Clinical Research Center (NIH RR 00722), and a pilot grant from the FM Kirby Center for Functional Brain Imaging at Kennedy Krieger Institute in Baltimore Maryland to GP.

1. Ahveninen J, Jaaskelainen IP, Pekkonen E, Hallberg A, Hietanen M, Naatanen R, Sillanaukee P. 2000. Global Field Power of Auditory N1 Correlates With Impaired Verbal-Memory Performance in Human Alcoholics. Neurosci Lett 285(2):131-4.
2. Calhoun VD, Adali T, McGinty V, Pekar JJ, Watson T, Pearlson GD. 2001. FMRI Activation In A Visual-Perception Task: Network Of Areas Detected Using The General Linear Model And Independent Components Analysis. NeuroImage 14(5):1080-8.
3. Calhoun, V. D., Golay, X., and Pearlson, G. D. 2000. Improved fMRI Slice Timing Correction: Interpolation Errors and Wrap Around Effects. In: Proc. ISMRM Denver, CO. 810 p.
4. Calhoun VD, Pekar JJ, McGinty VB, Adali T, Watson TD, Pearlson GD. 2002. Different Activation Dynamics in Multiple Neural Systems During Simulated Driving. Hum Brain Map 16(3):158-67.
5. Colarusso RP, Hammill DD. 1995. Motor-Free Visual Perception Test - Revised. Novato, CA: Academic Therapy Publications.
6. Colrain IM, Taylor J, McLean S, Buttery R, Wise G, Montgomery I. 1993. Dose Dependent Effects of Alcohol on Visual Evoked Potentials. Psychopharmacology (Berl) 112(2-3):383-8.
7. Conrod PJ, Peterson JB, Pihl RO, Mankowski S. 1997. Biphasic Effects of Alcohol on Heart Rate Are Influenced by Alcoholic Family History and Rate of Alcohol Ingestion. Alcohol Clin Exp Res 21(1):140-9.
8. Friston KJ, Fletcher P, Josephs O, Holmes A, Rugg MD, Turner R. 1998. Event-Related FMRI: Characterizing Differential Responses. NeuroImage 7(1):30-40.
9. Friston KJ, Holmes A, Poline JB, Price CJ, Frith CD. 1996. Detecting Activations in PET and FMRI: Levels of Inference and Power. NeuroImage 4(3 Pt 1):223-35.
10. Genovese CR, Lazar NA, Nichols T. 2002. Thresholding of Statistical Maps in Functional Neuroimaging Using the False Discovery Rate. Neuroimage 15(4):870-8.
11. George MS, Anton RF, Bloomer C, Teneback C, Drobes DJ, Lorberbaum JP, Nahas Z, Vincent DJ. 2001. Activation of Prefrontal Cortex and Anterior Thalamus in Alcoholic Subjects on Exposure to Alcohol-Specific Cues. Arch Gen Psychiatry 58(4):345-52.
12. Hiltunen AJ. 1997. Acute Alcohol Tolerance in Cognitive and Psychomotor Performance: Influence of the Alcohol Dose and Prior Alcohol Experience. Alcohol 14(2):125-30.
13. Janca A, Ustun TB, Sartorius N. 1994. New Versions of World Health Organization Instruments for the Assessment of Mental Disorders. Acta Psychiatr Scand 90(2):73-83.
14. Jones BM. 1973. Memory Impairment on the Ascending and Descending Limbs of the Blood Alcohol Curve. J Abnorm Psychol 82(1):24-32.
15. Kapur BM. 1989. Computer Blood Alcohol Calculator V1.20 ARF Software. Toronto, Canada: Addiction Research Foundation.
16. Kaszniak AW, Keyl PM, Albert MS. 1991. Dementia and the Older Driver. Hum Factors 33(5):527-37.
17. Keyl PM, Rebok GW, Gallo JJ. 1997. Screening Elderly Drivers in General Medical Setting: Toward the Development of a Valid and Feasible Assessment Procedure. AARP Andrus Foundation.
18. Kimura D. 2002. REVIEW. Sex Hormones Influence Human Cognitive Pattern. Neuroendocrinol Lett 23 Suppl 4:67-77.
19. Kourtzi Z, Bulthoff HH, Erb M, Grodd W. 2002. Object-Selective Responses in the Human Motion Area MT/MST. Nat Neurosci 5(1):17-8.

20. Krull KR, Smith LT, Sinha R, Parsons OA. 1993. Simple Reaction Time Event-Related Potentials: Effects of Alcohol and Sleep Deprivation. Alcohol Clin Exp Res 17(4):771-7.
21. Lamb MR, Robertson LC. 1987. Effect of Acute Alcohol on Attention and the Processing of Hierarchical Patterns. Alcohol Clin Exp Res 11(3):243-8.
22. Levin JM, Ross MH, Mendelson JH, Kaufman MJ, Lange N, Maas LC, Mello NK, Cohen BM, Renshaw PF. 1998a. Reduction in BOLD FMRI Response to Primary Visual Stimulation Following Alcohol Ingestion. Psychiatry Res 82(3):135-46.
23. Levin JM, Ross MH, Mendelson JH, Mello NK, Cohen BM, Renshaw PF. 1998b. Sex Differences in Blood-Oxygenation-Level-Dependent Functional MRI With Primary Visual Stimulation. Am J Psychiatry 155(3):434-6.
24. McGinty, V. B., Shih, R. A., Garrett, E. S., and Calhoun, V. D. 2001. Assessment of Intoxicated Driving with a Simulator: A Validation Study with on Road Driving. In: Proc. Human Centered Trans. Sim. Conf. Iowa City, IA.
25. Mungas D, Ehlers CL, Wall TL. 1994. Effects of Acute Alcohol Administration on Verbal and Spatial Learning. Alcohol Alcohol 29(2):163-9.
26. Nakamura K, Honda M, Okada T, Hankawa T, Fukuyama H, Konishi J, Shibasaki H. 2000. Attentional Modulation of Parieto-Occipital Cortical Responses: Implications for Hemispatial Neglect. J Neurol Sci 176(2):136-43.
27. Parker ES, Alkana RL, Birnbaum IM, Hartley JT, Noble EP. 1974. Alcohol and the Disruption of Cognitive Processes. Arch Gen Psychiatry 31(6):824-8.
28. Peterson JB, Rothfleisch J, Zelazo PD, Pihl RO. 1990. Acute Alcohol Intoxication and Cognitive Functioning. J Stud Alcohol 51(2):114-22.
29. Pfefferbaum A, Desmond JE, Galloway C, Menon V, Glover GH, Sullivan EV. 2001. Reorganization of Frontal Systems Used by Alcoholics for Spatial Working Memory: an FMRI Study. Neuroimage 14(1 Pt 1):7-20.
30. Raij T. 1999. Patterns of Brain Activity During Visual Imagery of Letters. J Cogn Neurosci 11(3):282-99.
31. Rebok GW, Bylsma FW, Keyl PM. 1990. The Effects of Alzheimer's Disease on Elderly Drivers. Gerontonol 30:194A.
32. Rebok GW, Keyl PM, Bylsma FW, Blaustein MJ, Tune L. 1994. The Effects of Alzheimer Disease on Driving-Related Abilities. Alzheimer Dis Assoc Disord 8(4):228-40.
33. Rosen LJ, Lee CL. 1976. Acute and Chronic Effects of Alcohol Use on Organizational Processes in Memory. J Abnorm Psychol 85(3):309-17.
34. Ryback RS. 1971. The Continuum and Specificity of the Effects of Alcohol on Memory. A Review. Q J Stud Alcohol 32(4):995-1016.
35. Schneider F, Habel U, Wagner M, Franke P, Salloum JB, Shah NJ, Toni I, Sulzbach C, Honig K, Maier W, Gaebel W, Zilles K. 2001. Subcortical Correlates of Craving in Recently Abstinent Alcoholic Patients. Am J Psychiatry 158(7):1075-83.
36. Sivak M, Olson PL, Kewman DG, Won H, Henson DL. 1981. Driving and Perceptual/Cognitive Skills: Behavioral Consequences of Brain Damage. Arch Phys Med Rehabil 62(10):476-83.
37. Stokx LC, Gaillard AW. 1986. Task and Driving Performance of Patients With a Severe Concussion of the Brain. J Clin Exp Neuropsychol 8(4):421-36.
38. Sugio T, Inui T, Matsuo K, Matsuzawa M, Glover GH, Nakai T. 1999. The Role of the Posterior Parietal Cortex in Human Object Recognition: a Functional Magnetic Resonance Imaging Study. Neurosci Lett 276(1):45-8.

39. Sullivan EV, Desmond JE, Lim KO, Pfefferbaum A. 2002a. Speed and Efficiency but Not Accuracy or Timing Deficits of Limb Movements in Alcoholic Men and Women. Alcohol Clin Exp Res 26(5):705-13.
40. Sullivan EV, Fama R, Rosenbloom MJ, Pfefferbaum A. 2002b. A Profile of Neuropsychological Deficits in Alcoholic Women. Neuropsychology 16(1):74-83.
41. Sullivan EV, Rosenbloom MJ, Pfefferbaum A. 2000. Pattern of Motor and Cognitive Deficits in Detoxified Alcoholic Men. Alcohol Clin Exp Res 24(5):611-21.
42. Talairach J, Tournoux P. 1988. A Co-Planar Sterotaxic Atlas of a Human Brain. Thieme, Stuttgart.
43. Tapert SF, Brown GG, Kindermann SS, Cheung EH, Frank LR, Brown SA. 2001. FMRI Measurement of Brain Dysfunction in Alcohol-Dependent Young Women. Alcohol Clin Exp Res 25(2):236-45.
44. Tarter RE, Arria AM, Van Thiel DH. 1991. Hepatic Encephalopathy Coexistent With Alcoholism. Recent Dev Alcohol 9:205-24.
45. Tarter RE, Jones BM. 1971. Absence of Intellectual Deterioration in Chronic Alcoholics. J Clin Psychol 27(4):453-5.
46. van de Moortele PF, Cerf B, Lobel E, Paradis AL, Faurion A, Le Bihan D. 1997. Latencies in FMRI Time-Series: Effect of Slice Acquisition Order and Perception. NMR Biomed 10(4-5):230-6.
47. Volkow ND, Mullani N, Gould L, Adler SS, Guynn RW, Overall JE, Dewey S. 1988. Effects of Acute Alcohol Intoxication on Cerebral Blood Flow Measured With PET. Psychiatry Res 24(2):201-9.
48. Wegner AJ, Gunthner A, Fahle M. 2001. Visual Performance and Recovery in Recently Detoxified Alcoholics. Alcohol Alcohol 36(2):171-9.
49. Woods RP. 1996. Modeling for Intergroup Comparisons of Imaging Data. NeuroImage 4(3 Pt 3):S84-S94.
50. Worsley KJ, Friston KJ. 1995. Analysis of FMRI Time-Series Revisited--Again. NeuroImage 2(3):173-81.
51. Wrase J, Grusser S, Klein S, Diener C, Hermann D, Flor H, Mann K, Braus D, Heinz A. 2002. Development of Alcohol-Associated Cues and Cue-Induced Brain Activation in Alcoholics. Eur Psychiatry 17(5):287.

Table 1: Individual accuracy rates and reaction times

	Sober		Intoxicated			Change	
Trial	Percent Correct	Median RT (sec)	Percent Correct	Median RT (sec)	BAC	Δ Percent Correct	Δ Median RT (sec)
Low dose	89±5	4.35±0.70	88±6	3.63±0.40	0.041±0.016	1±5	0.72±0.45
High dose	89±10	3.95±0.26	93±9	4.67±0.52	0.096±0.040	-4±7	-0.72±0.43

Table 2: Summary of areas detected in the main effects analysis

Area	Brodmann	L/R Volume (cc)	L/R Fixed Effects: Max T (x,y,z)
Sober (Max T=13.64)			
Lingual Gyrus	19,18,17	17.4/13.8	13.6(-21,-64,3)/13.0(21,-61,3)
Cuneus	17,18,19,30,23,7	17.4/16.4	12.1(-12,-75,8)/11.4(15,-78,18)
Precuneus	31,7,19	7.7/4.6	9.0(-15,-69,22)/9.9(24,-77,27)
Fusiform Gyrus	19,37,20,18	11.3/13.3	10.3(-21,-64,-5)/10.5(24,-64,-5)
Middle Occipital Gyrus	18,19,37	10.2/12.8	9.9(-12,-93,14)/10.8(27,-82,0)
Parahippocampal Gyrus	19,30,36,18,37,27,35,34,28	12.3/6.7	11.4(-24,-58,-1)/9.2(24,-53,-6)
Posterior Cingulate	30,31	4.6/2.6	10.9(-15,-61,8)/10.6(18,-67,8)
Cingulate Gyrus	32,24,9	5.1/2.0	6.7(-6,17,41)/4.5(12,20,45)
Superior Frontal Gyrus	8,6	3.1/3.1	8.2(-6,14,50)/7.8(6,9,55)
Middle Frontal Gyrus	9,6,8,46	4.1/10.2	4.4(-48,2,41)/8.1(50,5,37)
Medial Frontal Gyrus	6,8	3.1/2.6	6.9(0,0,60)/4.9(9,3,60)
Inferior Frontal Gyrus	45,9,47,13,44,46	5.1/8.2	5.6(-48,5,32)/6.9(36,26,3)
Thalamus		7.7/5.6	8.1(-6,-20,10)/6.8(12,-29,-3)
Precentral Gyrus	6,9,4	2.0/7.2	5.2(-30,-9,56)/6.8(36,-6,56)
Inferior Parietal Lobule	40	0.5/4.6	3.1(-33,-38,48)/5.3(42,-38,48)
Superior Parietal Lobule	7	1.5/4.6	4.7(-21,-68,45)/5.2(24,-65,40)
Middle Temporal Gyrus	19,39,37	3.1/2.0	4.9(-42,-80,22)/6.6(42,-78,18)
Low Dose (Max T=11.49)			
Lingual Gyrus	18,19,17	12.8/11.3	10.6(-21,-70,3)/11.5(27,-76,0)
Cuneus	18,23,17,19,30,7	13.8/13.3	9.2(-15,-72,13)/9.4(24,-83,27)
Precuneus	7,31,19,18	6.1/7.2	7.2(-21,-71,40)/8.6(27,-68,36)
Fusiform Gyrus	37,19,20	9.2/12.3	7.7(-21,-59,-5)/10.4(36,-50,-10)
Middle Occipital Gyrus	18,19,37	8.7/10.8	8.0(-27,-80,22)/11.0(27,-87,18)
Parahippocampal Gyrus	19,30,18,37,36,28,35,34,27	7.7/7.7	6.3(-15,-32,-3)/8.8(30,-56,-6)
Posterior Cingulate	30,31,18	3.6/2.0	7.6(-18,-66,17)/7.6(24,-61,8)
Cingulate Gyrus	32,24	2.6/1.5	5.4(-12,20,40)/7.4(12,17,45)
Superior Frontal Gyrus	6,8	2.6/3.6	6.0(-3,11,50)/9.3(9,11,50)
Middle Frontal Gyrus	6,9,46,10	4.1/9.7	5.5(-27,-3,51)/8.1(30,0,51)
Medial Frontal Gyrus	32,6,8,9	1.5/3.6	7.8(-9,14,45)/5.7(9,3,55)
Inferior Frontal Gyrus	9,45,47,44,46,13,11	6.1/7.7	5.7(-48,7,27)/7.8(45,10,27)
Thalamus		4.1/4.1	5.6(-21,-29,1)/5.8(12,-26,-3)
Precentral Gyrus	9,6	1.5/1.5	4.0(-45,5,37)/5.2(42,5,37)
Inferior Parietal Lobule	40	2.0/6.1	4.6(-33,-38,48)/5.8(33,-44,48)
Superior Parietal Lobule	7	2.6/4.1	4.1(-15,-55,63)/7.9(24,-68,45)
Middle Temporal Gyrus	19,39,37	2.6/2.6	7.1(-39,-78,18)/6.2(42,-69,13)
R Insula		3.6	5.2(33,23,3)
Postcentral Gyrus	5,7,2,1,3,40	1.5/3.6	2.9(-18,-49,67)/4.5(33,-44,57)
High Dose (Max T=7.56)			
Lingual Gyrus	18,19,17,30	10.8/14.3	6.8(-21,-61,-1)/7.6(21,-73,-1)
Cuneus	23,7,17,18,30,19	7.7/9.7	6.6(-12,-70,8)/6.2(15,-75,13)
Precuneus	7,31,19	4.1/3.6	5.5(-21,-66,26)/5.0(18,-74,27)
Fusiform Gyrus	19,37,20	7.2/6.1	5.7(-27,-41,-11)/7.5(27,-56,-6)
Middle Occipital Gyrus	18,19,37	3.6/8.7	3.7(-12,-90,14)/4.5(24,-90,14)
Parahippocampal Gyrus	19,30,36,37,27,35,28	8.2/5.6	6.1(-27,-50,-6)/6.2(24,-50,-2)

Posterior Cingulate	30,31	3.1/1.5	7.3(-18,-64,8)/5.9(21,-61,8)
Cingulate Gyrus	32,24	4.1/3.1	4.3(-9,19,36)/3.9(12,2,46)
Superior Frontal Gyrus	6,8,9	1.5/2.6	4.1(-6,11,55)/3.0(9,9,59)
Middle Frontal Gyrus	6,9,46	0.5/3.1	2.9(-42,19,22)/3.3(30,0,51)
Medial Frontal Gyrus	6,32,8,9	3.1/5.6	5.3(-9,14,45)/5.6(9,8,50)
Inferior Frontal Gyrus	9,44,13,47,45,46	2.6/10.8	3.7(-39,21,8)/4.7(50,4,27)
Thalamus		3.1/5.1	5.9(-6,-29,1)/5.7(12,-29,1)
Precentral Gyrus	6,9,4,44	2.0/6.1	3.2(-48,-1,41)/4.4(53,2,37)
Insula	13	2.6/2.6	3.0(-33,-23,15)/3.0(42,-15,-3)

Table 3: Summary of areas detected in the correlation analysis

Area	Brodmann	L/R Volume (cc)	L/R Random Effects: Max T (x,y,z)
Positive (Dose Dependent Decreases)			
Precuneus	7,19,39,31	3.6/3.6	4.0(-18,-59,49)/3.9(30,-65,31)
Superior Parietal Lobule	7	1.6/2.0	3.6(-21,-62,45)/3.6(18,-52,58)
Middle Frontal Gyrus	6,11,8,47,10	2.1/1.6	3.2(-39,46,-11)/3.5(27,-1,46)
Middle Temporal Gyrus	39,37,19,22,20,21	1.6/1.3	3.4(-36,-69,26)/3.2(45,-55,3)
Middle Occipital Gyrus	19,18,37	1.4/1.5	3.3(-33,-75,18)/2.6(30,-87,18)
Anterior Cingulate	24,32,10	1.5/0.2	3.2(-6,26,-1)/2.2(0,29,3)
Posterior Cingulate	23,30,29,31	0.5/0.4	3.2(-3,-42,25)/2.5(6,-40,25)
Inferior Parietal Lobule	7,40,39	0.9/0.7	3.0(-30,-56,44)/2.5(33,-42,44)
(lateral) Superior Frontal Gyrus	11,6,8,10	0.8/0.9	3.0(-36,46,-11)/2.6(21,31,44)
Posterior Cingulate Gyrus	31,32,24	1.6/0.2	2.5(0,-42,25)/2.0(12,-45,25)
Medial Frontal Gyrus	32,6,10,8	0.5/0.3	2.5(-21,11,41)/2.0(15,9,55)
Fusiform Gyrus	37,20	0.7/0.4	2.3(-42,-38,-11)/2.4(42,-56,-6)
Negative (Dose Dependent Increases)			
(medial) Superior Frontal Gyrus	8,6,9	1.5/0.8	4.2(0,38,53)/4.4(3,38,53)
R Precentral Gyrus	6,4,43	4.0	3.8(45,-3,51)
Medial Frontal Gyrus	8,9,6,32	0.6/0.4	2.8(0,49,39)/3.2(3,49,39)
R Superior Temporal Gyrus	22,13,29,41	1.0	2.8(45,-17,1)
R Insula	13	1.5	2.8(39,-28,15)
L Superior Parietal Lobule	7	0.2	2.5(-42,-56,53)
Postcentral Gyrus	3,5,43,1	0.2/1.0	2.3(-36,-46,62)/2.4(45,-15,56)
L Inferior Parietal Lobule	40	0.9	2.3(-45,-53,49)
L Cingulate Gyrus	24	0.2	2.3(-3,-1,46)

Figure 1: Timeline of the MVPT-R fMRI Paradigm

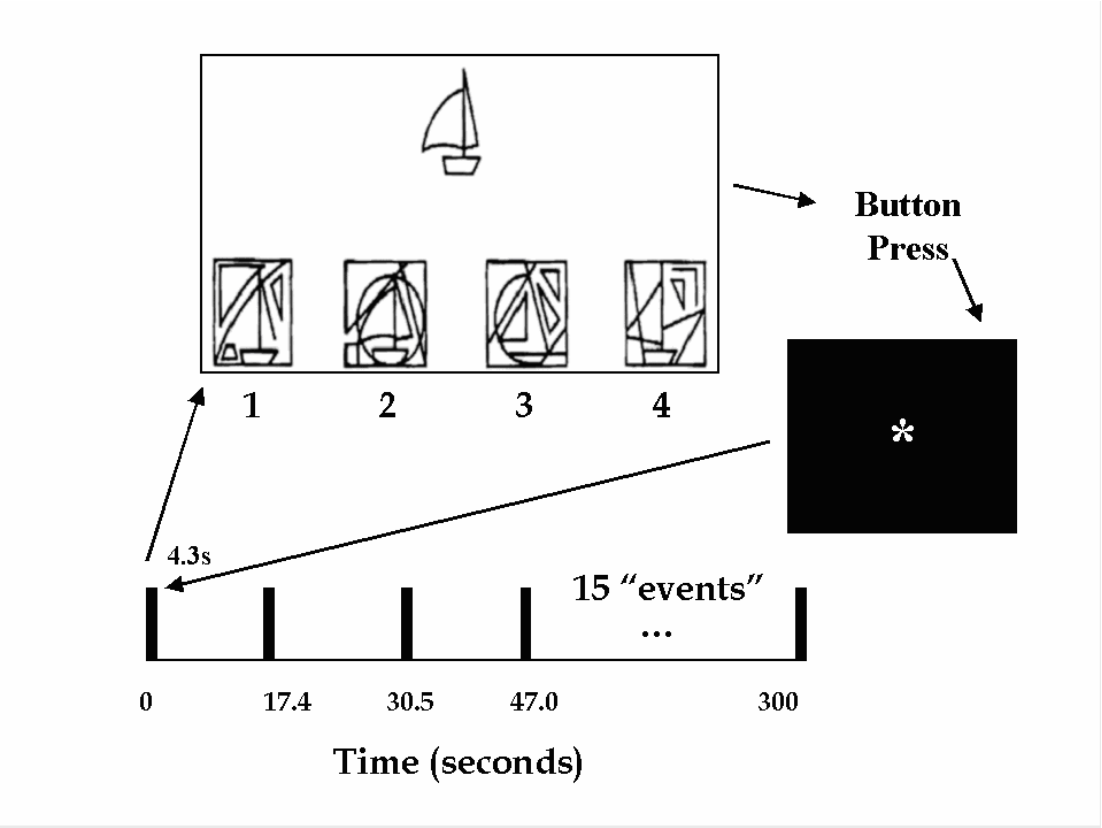

Figure 2: Main effect group maps for (mean) sober, low dose, and high dose conditions

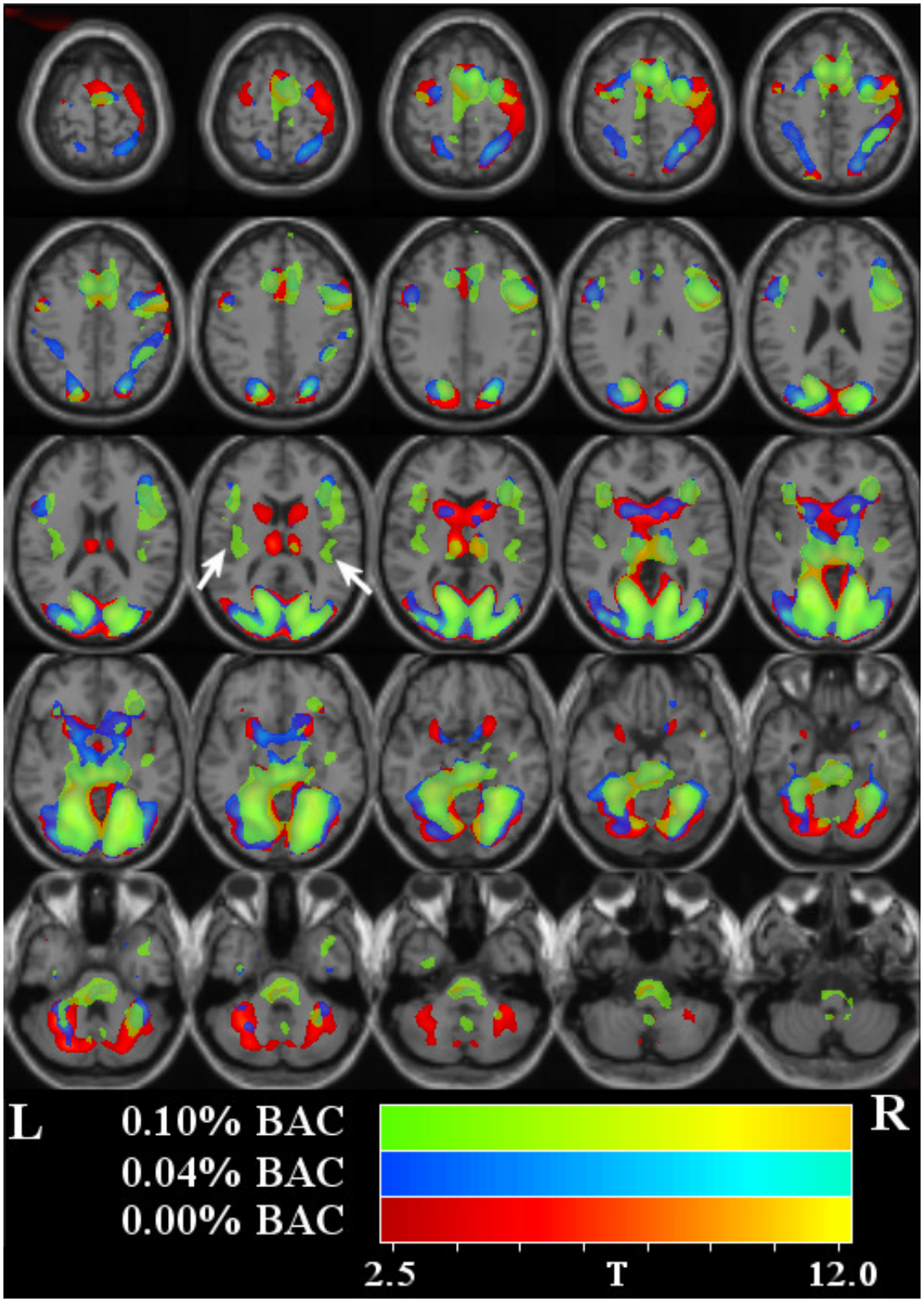

Figure 3: Graphical view of CNR differences detected in the main effects analysis

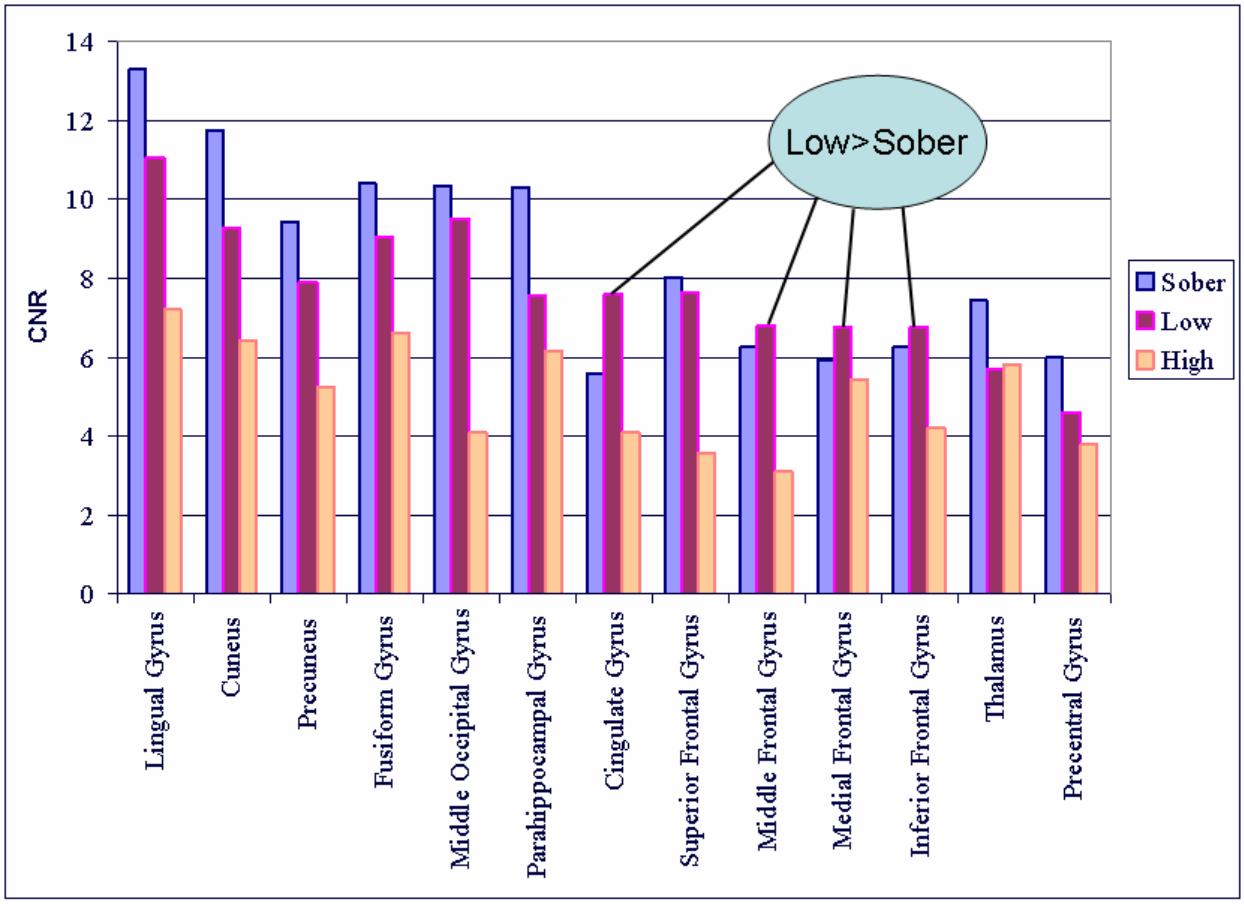

Figure 4: EtOH blood alcohol content correlation maps and plot

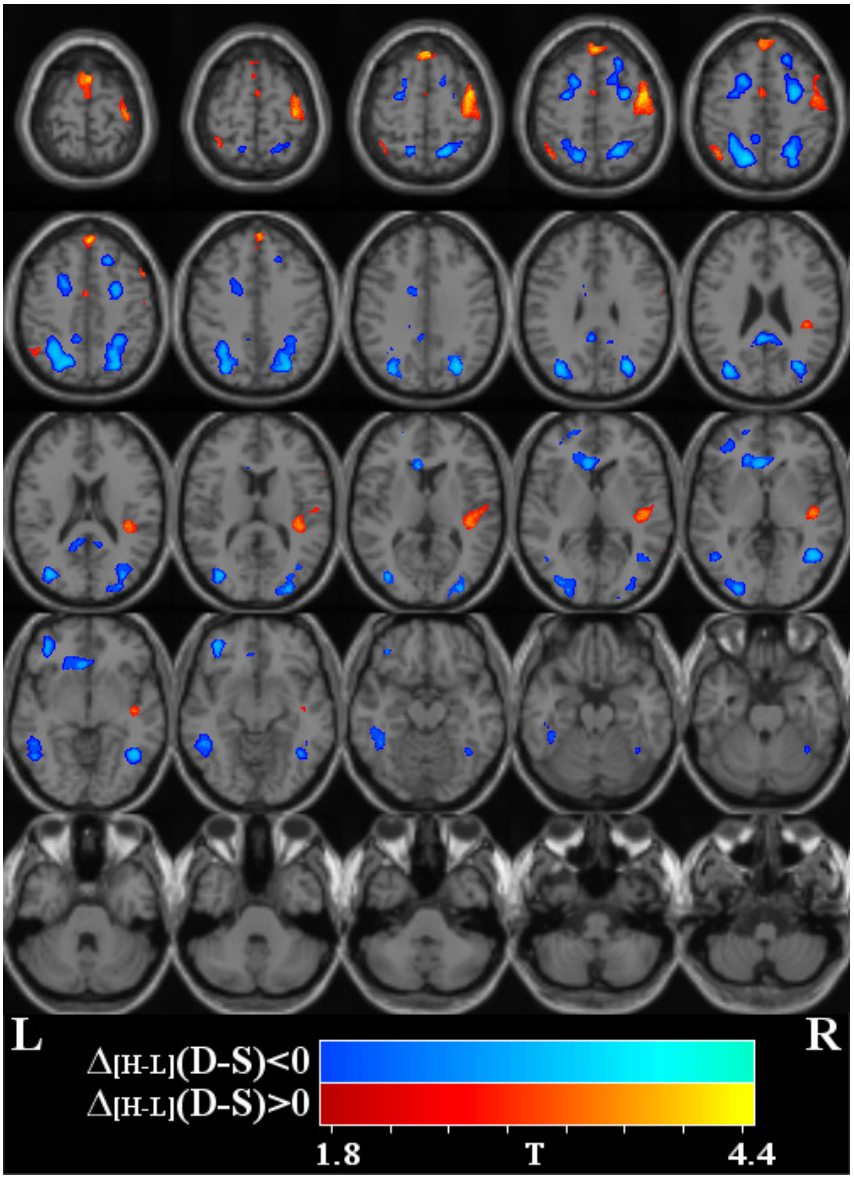

Figure Legends

Figure 1: Timeline of the MVPT-R fMRI Paradigm

The participants were asked to indicate which of the four lower figures contained the upper figure by pressing 1, 2, 3, or 4. The correct answer for this figure is 2.

Figure 2: Main effect group maps for (mean) sober, low dose, and high dose conditions

T-maps are displayed over the T_1-weighted template. Images were thresholded at $p < 0.05$ (corrected for multiple comparisons). All colored regions in the figure represent activations, and are color-coded to discriminate the alcohol dosing level. The main effect SPM group analysis for 1) (mean) sober (colored red/orange), 2) low dose (colored blue/cyan), and 3) high dose (colored green/yellow) are displayed on the same image for clarity. Alcohol dose results in a global decrease in contrast-to-noise and also that there are some localized increases and decreases.

Figure 3: Graphical view of CNR differences detected in the main effects analysis

Bar graph comparison of CNR-by-area in the (mean) sober, low dose, and high dose studies. Visual areas demonstrate a clear dose dependent decrease in CNR whereas frontal regions appear to be higher in the low dose condition and then lower in the high dose condition.

Figure 4: EtOH blood alcohol content correlation maps and plots

Comparison of the amplitude difference between the sober (S) and drug (D) conditions for the high (H) dose with the amplitude difference between the sober and intoxicated conditions for the low (L) dose, that is ($\Delta_{H\pm L}[D\text{-}S]$). *T*-maps are displayed over one of the normalized EPI images. Images were thresholded at $p<0.05$ and a cluster size of 50 voxels. Dose dependent decreases are depicted in blue/cyan whereas dose dependent increases are depicted in red/orange.

Table 1: Individual accuracy rates and reaction times

Average duration (in seconds) the participants took to determine the matching figure along with accuracy results for the two sober conditions, the low dose condition, and the high dose condition. Scores were within 5% of the norm for the MVPT-R test. Participants receiving the Low dose of alcohol tended ($p<0.07$) towards slightly decreased reaction time whereas participants receiving the high dose of alcohol slightly ($p<0.08$) increased in reaction time.

Table 2: Summary of areas detected in the main effects analysis

A selection of areas detected by the analysis of main effect (determined by selecting a local statistical maximum within each region) along with their Talairach coordinates. Voxels above the threshold were converted to Talairach coordinates and entered into a database to provide anatomic and functional labels for the left (L) and right (R) hemispheres. The volume of activated voxels in each area is provided in cubic centimeters (cc). Within each area, the maximum *t* value and its coordinate are provided.

Table 3: Summary of areas detected in the correlation analysis

A selection of areas detected by the correlation-with-dose analysis (determined by selecting a local statistical maximum within each region) along with their Talairach coordinates. Voxels above the threshold were converted to Talairach coordinates and entered into a database to provide anatomic and functional labels for the left (L) and right (R) hemispheres. The volume of activated voxels in each area is provided in cubic centimeters (cc). Within each area, the maximum *t* value and its coordinate are provided.